

Mössbauer Effect for Fe<sup>57</sup> in Ferroelectric Lead Titanate

V. G. Bhide and M. S. Hegde

*National Physical Laboratory, New Delhi-12, India*

(Received 2 June 1971)

Mössbauer effect for Fe<sup>57</sup> in ferroelectric PbTiO<sub>3</sub> has been investigated over the temperature range 300–1100 °K. The quadrupole interaction in the ferroelectric phase remains nearly saturated up to 320 °C, beyond which it decreases gradually to disappear at and above the transition temperature  $T_C = (480 \pm 2)^\circ\text{C}$ . The ratio of the quadrupole interaction sensed by the  $\frac{5}{2}$  state of Fe<sup>57</sup> nucleus in PbTiO<sub>3</sub> to that in BaTiO<sub>3</sub> at room temperature is  $1.41 \pm 0.04$ , in good agreement with the value  $1.46 \pm 0.07$  obtained through perturbed Sc<sup>44</sup>  $\gamma$ - $\gamma$  angular-correlation studies by Hass and Glass. The numerical value of the electric field gradient, as also that of isomer shift at room temperature, indicates that this lattice is more covalent than BaTiO<sub>3</sub>. Both the center shift and the area under resonance show anomalous temperature variation in the vicinity of the transition temperature. Analysis of the temperature variation of these parameters suggests that the Debye temperature of the lattice decreases considerably on crossing the transition temperature. Analytical form of the Lamb-Mössbauer factor in the presence of the Cochran type of soft mode has been derived. Computer fitting of the theoretical value of the Lamb-Mössbauer factor at various temperatures normalized to that at  $T_C$ , with the corresponding normalized areas under resonance, has brought out the essential validity of the suggested temperature variation of the soft mode.

## I. INTRODUCTION

Although lead titanate is isomorphous with BaTiO<sub>3</sub> and undergoes a ferroelectric phase transition at about 490 °C, it differs from barium titanate in a number of respects.<sup>1</sup> First of all, unlike barium titanate, lead titanate does not undergo any other phase transition at lower temperatures.<sup>2</sup> Second, birefringence  $n_c - n_a$  (difference in the refractive index  $n$  along the  $c$  and  $a$  axes, respectively) in lead titanate has an anomalous temperature dependence<sup>3</sup> inasmuch as  $n_c - n_a$  increases (absolutely) initially with temperature, reaches a maximum at about 400 °C, and then decreases to disappear at and above the ferroelectric phase-transition temperature. Third, the coercive field<sup>4</sup> in lead titanate below 300 °C is more than the dielectric breakdown field, with the result that it is difficult to observe the  $P$ - $E$  hysteresis loop. It is essentially because of this fact that lead titanate behaves as a "frozen" ferroelectric and it has not been possible to study the temperature variation of the spontaneous polarization. Fourth, the tetragonal strain in this lattice<sup>5</sup> is nearly 6% as opposed to 1% in barium titanate.<sup>6</sup> In view of these peculiar properties and also the high transition temperature, lead titanate offers an interesting system to study. The relatively little information that is available with lead titanate has essentially been due to the difficulty in growing single crystals of this material. We have described in previous papers<sup>7,8</sup> a method of growing single crystals of PbTiO<sub>3</sub>. With this method it has been possible to obtain small flakes of single-crystal lead titanate. The study of dielectric characteristics of these crystals showed that  $T_C$  is equal to

$(490 \pm 5)^\circ\text{C}$  and in the paraelectric phase the dielectric constant could be well described by the Curie-Weiss law with the Curie constant  $C = (1.1 \times 10^5)^\circ\text{C}$ . Recently, Remeika and Glass<sup>9</sup> have developed a method for growing large crystals of PbTiO<sub>3</sub>. Using these crystals, Shirane *et al.*<sup>10</sup> reported the transition temperature of  $(492 \pm 5)^\circ\text{C}$  and  $C = (4.1 \times 10^5)^\circ\text{C}$  with  $T_0 = 449^\circ\text{C}$ . While we had iron impurity in our crystals, the crystals investigated by Shirane *et al.* had UO<sub>3</sub> impurities. The difference in the  $C$  values may possibly be due to different impurities in the crystal.

In these ABO<sub>3</sub>-type perovskite ferroelectrics it has been shown that at the ferroelectric transition temperature they undergo a displacement transition associated with the  $B^{4+}$  ion shift towards one of the oxygen ions in the  $BO_6$  octahedra. A consequence of this displacement is the variety of domain patterns<sup>11</sup> which these crystals exhibit. Further, the loss of center of symmetry involved in the displacement of the  $B^{4+}$  ion creates an electric field gradient (EFG) at the  $B$  site, which can be investigated through Mössbauer spectroscopy if the  $B$  ion is a Mössbauer isotope or if it could be replaced by a Mössbauer isotope without affecting the ferroelectric properties. Such a study will not only give information on the temperature variation of the EFG but will throw some light on the variation of the spontaneous polarization and thus provide a clue to the anomalous temperature variation of the birefringence. What is still more important and basic from the point of view of ferroelectricity in these crystals is a possibility of investigating the temperature variation of the soft optic mode responsible for the ferroelectric transition through the temper-

ature variation of the Lamb-Mössbauer factor. Our earlier investigation<sup>12,13</sup> has brought out clearly the usefulness of the Mössbauer-effect technique in the study of ferroelectric properties of BaTiO<sub>3</sub>. The soft modes in BaTiO<sub>3</sub> are highly damped<sup>14</sup> and extremely anisotropic,<sup>15</sup> unlike in SrTiO<sub>3</sub> and KTaO<sub>3</sub>, where they are much more well defined. Although the soft modes in PbTiO<sub>3</sub> are expected to be still more highly damped because of the higher Curie temperature, the recent inelastic neutron study by Shirane *et al.*<sup>10</sup> has surprisingly shown that the soft modes in PbTiO<sub>3</sub> are fairly well defined and follow the Curie-Weiss law when approached from the high-temperature side. However, the soft-mode behavior quite close to  $T_C$  is difficult to infer because of the inadequacy of resolution of the broad neutron group corresponding to  $\vec{q} = 0$  modes. The Lamb-Mössbauer factor, on the other hand, is sensitive to finer details of the mode behavior. As we shall see, our Mössbauer studies have shown the existence of the soft mode through the  $f$ -factor measurements. The comparison of the analytical form of the temperature variation has essentially brought out the fact that the soft mode has a temperature dependence predicted by Cochran. In addition, these studies have shown that the Debye temperature of the lattice as seen by the Mössbauer probe decreases considerably on going through the transition as approached from the lower-temperature side. The temperature variation of the center shift has provided a useful check on the conclusions drawn from the  $f$ -factor measurements. These studies have, in addition, provided some information on the polarization behavior through the temperature variation of the quadrupole interaction and on the nature of the chemical bond through the isomer shift.

## II. EXPERIMENTAL

For Mössbauer studies of ferroelectric lead titanate it would have been ideal, had titanium itself been a Mössbauer isotope. In the absence of this possibility one can either use PbTiO<sub>3</sub>:Co<sup>57</sup> sources or Fe<sup>57</sup>-doped PbTiO<sub>3</sub> absorbers. For a variety of reasons the use of the Fe<sup>57</sup>-doped PbTiO<sub>3</sub> absorber is not desirable. In the first instance, one would need to have at least 0.1 mg/cm<sup>2</sup> of Fe<sup>57</sup> in the absorber so as to have good absorption. This concentration of iron is expected to have a considerable poisoning effect on the ferroelectric properties of PbTiO<sub>3</sub> in much the same way as it has on the ferroelectric properties of isomorphous BaTiO<sub>3</sub>.<sup>16</sup> Second, the use of PbTiO<sub>3</sub>:Fe<sup>57</sup> absorbers is not advisable because the Pb absorption would cause a small signal-to-noise ratio in the resonance spectra. In contrast, in the PbTiO<sub>3</sub>:Co<sup>57</sup> source the impurity content is extremely small and is not expected to affect the ferroelectric properties

of PbTiO<sub>3</sub>. In view of these considerations, we used in the present investigation Co<sup>57</sup>-doped sources matched against a (i) 310-enriched-stainless-steel absorber and (ii) K<sub>4</sub>Fe(CN)<sub>6</sub>·3H<sub>2</sub>O single-crystal absorber (hereafter referred to as 310 ESS and KFCT, respectively).

PbTiO<sub>3</sub> was synthesized by solid-state reaction between PbO and TiO<sub>2</sub> (A. R. grade) at about 800 °C. The homogeneity of the sample was tested by x rays. A few drops of aqueous solution of Co<sup>57</sup>Cl<sub>2</sub> were dried on the surface of a sintered thin disk of PbTiO<sub>3</sub>. The disk was then heated at 1000 °C in a platinum boat for 1 h in PbO-saturated vapor to accomplish thermal diffusion of the activity. The presence of a PbO atmosphere during thermal diffusion of Co<sup>57</sup> is essential to compensate for the PbO loss that occurs because of the dissociation of PbTiO<sub>3</sub>. The preparation of a source is indeed a tricky problem, and if the PbO vapor pressure is not maintained at the proper level, various defect structures arise. The Mössbauer effect in these defect structures is discussed in a separate communication.<sup>17</sup> The use of a single crystal of PbTiO<sub>3</sub> for the preparation of the source does not provide any particular advantage for the following reasons. Since PbTiO<sub>3</sub> behaves as a "frozen" ferroelectric, control of domain structure in PbTiO<sub>3</sub> by the bias field is not possible as in BaTiO<sub>3</sub>. Second, in a single-crystal specimen we find it extremely difficult to maintain stoichiometry during thermal diffusion of the activity.

Mössbauer data were collected in transmission geometry by matching the Co<sup>57</sup>-doped PbTiO<sub>3</sub> source against the KFCT single-crystal absorber and also against 310 ESS. A relative velocity was imparted to the absorbers using a conventional constant-velocity mechanical drive reported earlier.<sup>12</sup> The spectra were taken over the temperature range 300 to 1100 °K using a suitably designed high-temperature furnace. The temperature in the furnace could be maintained at the desired value to within ± 2 °C. In the temperature range up to 650 °K, the KFCT absorber was used with advantage. With this absorber one obtained well-resolved quadrupole-split spectra. From this series, the line positions, the center shift, and the quadrupole interaction could be computed without ambiguity. Since absorption with the KFCT absorber was small we had to use the 310 ESS absorber in the high-temperature region. With the 310 ESS absorber, although the absorption was large, one obtained a broad resonance with a linewidth much greater than the characteristic linewidth of the absorber (when matched against a standard single-line source), indicating unresolved quadrupolar interaction. The linewidth of the spectra decreased on increasing the temperature, and above  $T_C$  the linewidth  $2\Gamma = 0.70$  mm/sec ( $\Gamma$  is the half-width at half-maximum) was equal

to the characteristic width of the absorber, indicating the disappearance of the quadrupolar interaction. The unresolved spectra below  $T_C$  were resolved by fitting two Lorentzians of width  $2\Gamma = 0.70$  mm/sec with varying intensities and line positions. In the temperature range where spectra were obtained with both KFCT and 310 ESS, the quadrupole interaction obtained by resolving the ESS spectra agreed closely with those obtained with KFCT. In the temperature range below  $650^\circ\text{K}$ , the quadrupole interaction and isomer shift were computed from the KFCT series with an accuracy of  $\pm 0.02$  mm/sec, whereas in the temperature range above  $650^\circ\text{K}$  the quadrupole interaction and center shifts could be computed to an accuracy of  $\pm 0.04$  mm/sec.

In studies where the lattice under investigation is used as a source, and more particularly when  $\text{Co}^{57}$  or  $\text{Fe}^{57}$  is not part of the host lattice, the questions regarding the valence state and the site location of the Mössbauer probe need be considered before the data are interpreted. Extensive studies on the magnetic susceptibility,<sup>18</sup> dielectric properties, optical absorption,<sup>19</sup> electron paramagnetic resonance (EPR),<sup>20,21</sup> and Mössbauer data<sup>12,13,22</sup> have shown that both Co and Fe impurities occupy the  $\text{Ti}^{4+}$  site in both  $\text{BaTiO}_3$  and  $\text{SrTiO}_3$ . Since  $\text{PbTiO}_3$  is isomorphous, it is expected that Co and Fe impurities in this lattice will also occupy the  $\text{Ti}^{4+}$  site. Ionic size considerations proposed by Muller<sup>20</sup> strongly support this conclusion. The most direct evidence is, however, available from the EPR studies which have shown the existence of  $\text{Fe}^{3+}$  at the  $\text{Ti}^{4+}$  site in  $\text{PbTiO}_3$ .<sup>23</sup> Taking for granted that Co as well as Fe impurities substitute for the  $\text{Ti}^{4+}$  ion in this lattice, the next question that needs to be considered is, what is the equilibrium electronic state of Co and Fe impurities as well as Fe formed out of the electron-capture decay of  $\text{Co}^{57}$  in this lattice? Unlike in  $\text{SrTiO}_3$ ,<sup>22</sup> both Co and Fe impurities exist in the high-spin state in  $\text{PbTiO}_3$ . Thus there is no complication arising out of the electron-capture decay of  $\text{Co}^{57}$  in this lattice, i.e., Fe impurity doped as such as well as Fe formed out of the electron-capture decay of  $\text{Co}^{57}$  will be in high-spin trivalent state ( $\text{Fe}^{3+}$ ).

### III. RESULTS AND DISCUSSION

#### A. Isomer Shift and Center Shift

In all, three data runs were made in the range  $300$ – $1100^\circ\text{K}$ , using a 310 ESS absorber. The resonance spectra obtained at close intervals over the entire range were similar in all the runs. Figure 1 shows some typical spectra obtained with this absorber. The spectra with this absorber show a two-line composite spectrum below the transition temperature  $T_C$ . In order to check on the resolution of the composite spectra a few runs were made

over the temperature region up to  $650^\circ\text{K}$  using KFCT. Typical spectra obtained with this absorber are shown in Fig. 2. These spectra showed two well-resolved resonance dips of equal intensity. In the room-temperature spectrum, these dips are located at  $0.00 \pm 0.02$  and  $0.65 \pm 0.02$  mm/sec. For a variety of reasons these spectra are attributed to

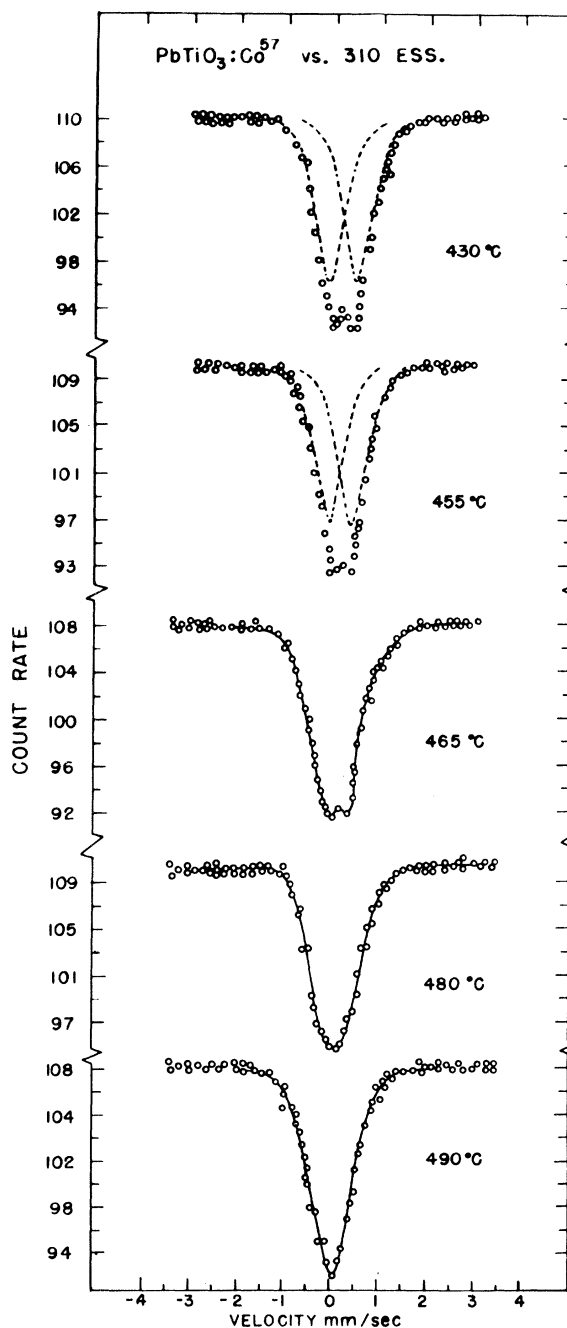


FIG. 1. Typical spectra for  $\text{PbTiO}_3:\text{Co}^{57}$  source matched against 310 ESS absorber at various temperatures.

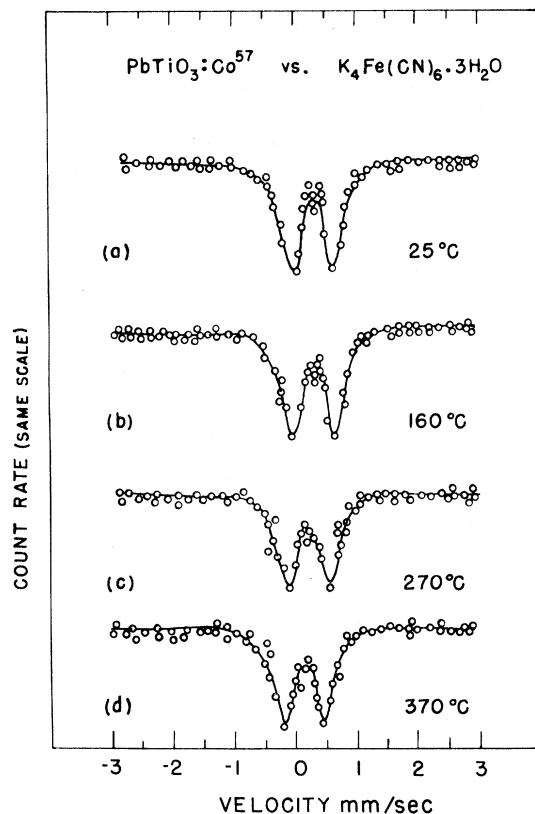


FIG. 2. Typical spectra for  $\text{PbTiO}_3:\text{Co}^{57}$  source matched against  $\text{K}_4\text{Fe}(\text{CN})_6 \cdot 3\text{H}_2\text{O}$  single-crystal absorber at various temperatures.

$\text{Fe}^{3+}$  ( $3d^5$ ,  ${}^6S_{5/2}$ ) at the  $\text{Ti}^{4+}$  site. The line positions derived from the KFCT-absorber series helped in the resolution of the composite spectra obtained with the 310 ESS absorber over the entire temperature range. From these series of spectra, the center shift, quadrupole interaction, and the area under the resonance curve were computed following usual methods.

The isomer shift at room temperature is  $0.38 \pm 0.02$  mm/sec (with respect to the 310 ESS), whereas the quadrupole interaction at room temperature is  $0.65 \pm 0.02$  mm/sec. It is clearly seen from both series that the two partners of the split spectrum come closer (above  $320^\circ\text{C}$ ) as the temperature is raised and merge into a single resonance with characteristic linewidth of the absorber at and above the transition temperature. The transition temperature could be located from the variation of the quadrupole interaction and the area under resonance as a function of temperature. The transition temperature can also be located, as we shall see later, from the anomalous variation of the center shift, as also from the dip in the Lamb-Mössbauer factor. The transition temperature determined from any one of these methods was

found to be  $(480 \pm 2)^\circ\text{C}$ . The disappearance of the splitting above  $T_c$ , equal intensity of the two resonances over the entire temperature range, and the location of the center of gravity of the spectrum lead us to assign unequivocally the series of spectra to  $\text{Fe}^{3+}$  at the  $\text{Ti}^{4+}$  site. In addition, these results also indicate that the Mössbauer probe is seeing the perfect-lattice local environment.

It is significant to point out that the observed isomer shift in lead titanate is lower than that in  $\text{BaTiO}_3$ . This is indeed expected because the displacement of the  $\text{Ti}^{4+}$  ion towards one of the oxygen ions ( $\text{Ti}-\text{O}_I$ ) in the  $\text{TiO}_6$  octahedra in  $\text{PbTiO}_3$  is much greater<sup>3</sup> than it is in  $\text{BaTiO}_3$ . Simanek and Sroubek's<sup>24</sup> interpretation of the covalency effects in a high-spin  $\text{Fe}^{3+}$  ion surrounded by an oxygen octahedron also show that the isomer shift is sensitive to the bond length and overlap of the  $2p$  orbitals with the  $4s$  orbitals of the central Fe ion. Figure 3 shows the variation of the center shift as a function of temperature. From this variation it can be clearly seen that the center shift changes abruptly at the transition temperature. We might now analyze whether this abrupt change in the center shift is due to sudden changes in the isomer shift (IS) and/or to the discontinuous change in the second-order Doppler shift (SOD) at the transition temperature. Since the present study relates to the absorber maintained at a constant temperature, the observed changes in the center shift reflect changes in the energy levels of the  $\text{Fe}^{57}$  nucleus in the source as a function of temperature. The center shift  $\delta E_{\text{total}}$  is made up of two contributions,

$$\delta E_{\text{total}} = \delta E_{\text{IS}} + \delta E_{\text{SOD}}, \quad (1)$$

where  $\delta E_{\text{IS}}$  is the shift due to isomer shift and  $\delta E_{\text{SOD}}$  is the shift due to second-order Doppler effect. Both these contributory factors have either an explicit or implicit temperature dependence. The

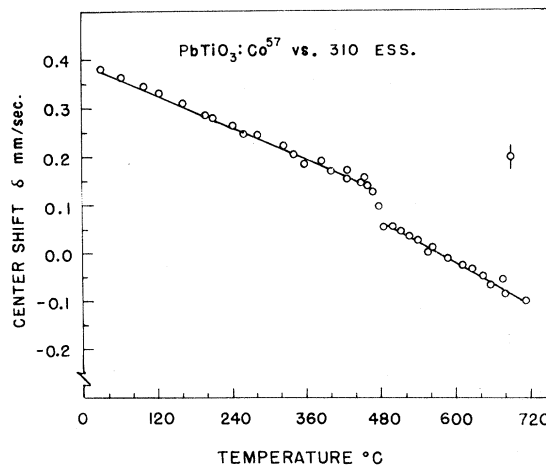


FIG. 3. Variation of the center shift with temperature.

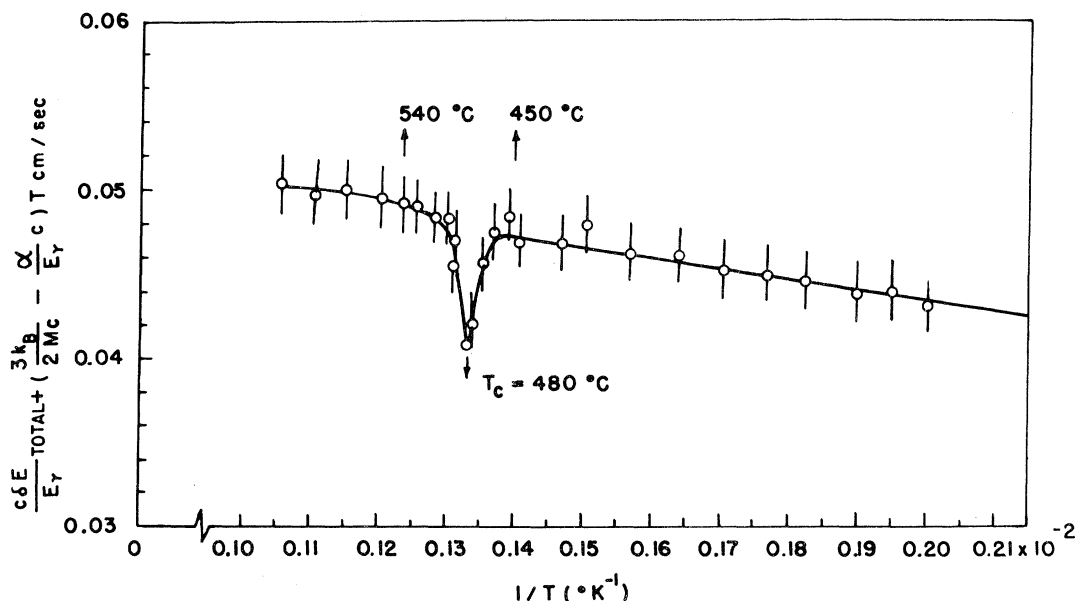


FIG. 4. Plot of  $c\delta E_{\text{total}}/E_{\gamma} + [3k_B/2Mc - (\alpha/E_{\gamma})c]T$  against the reciprocal of temperature ( $^{\circ}\text{K}^{-1}$ ), showing clearly an anomaly in the vicinity of  $T_C$ .

temperature dependence of  $\delta E_{\text{IS}}$  arises out of the thermal expansion consequent on increasing the temperature. In the high-temperature region one can write

$$\delta E(T)_{\text{IS}} = \delta E(0)_{\text{IS}} + \alpha T, \quad (2)$$

where  $\alpha$  is a constant which can be evaluated from the knowledge of thermal expansion and the pressure dependence of the isomer shift. The changes in  $\delta E_{\text{SOD}}$  as a function of temperature are essentially caused by the variation of the mean-square velocity as a function of temperature. In the region  $T > \frac{1}{3}\Theta_D$  one can express  $\delta E(T)_{\text{SOD}}$  as follows<sup>25</sup>:

$$\frac{\delta E(T)_{\text{SOD}}}{E_{\gamma}} = \frac{3k_B T}{2Mc^2} \left(1 + \frac{\Theta_D^2}{20T^2}\right), \quad (3)$$

where  $E_{\gamma}$  is the  $\gamma$ -ray energy,  $M$  is the mass of the nucleus,  $k_B$  is the Boltzmann constant,  $T$  and  $\Theta_D$  are ambient and Debye temperatures (in  $^{\circ}\text{K}$ ), respectively. Combining (1)–(3), one can write

$$\frac{\delta E(T)_{\text{total}}}{E_{\gamma}} + \left(\frac{3k_B}{2Mc^2} - \frac{\alpha}{E_{\gamma}}\right)T = \frac{\delta E(0)_{\text{IS}}}{E_{\gamma}} - \frac{3k_B\Theta_D^2}{40Mc^2T}. \quad (4)$$

If we plot the left-hand side of Eq. (4) as a function of  $1/T$ , then the intercept will give  $\delta E(0)_{\text{IS}}/E_{\gamma}$  and the slope of the plot will yield the Debye temperature. Following Pound *et al.*<sup>26</sup> and Pipkorn *et al.*<sup>27</sup> if we assume that 4s atomic wave functions of the  $\text{Fe}^{3+}$  ion are changed because of thermal expansion, then using Danon's<sup>28</sup> recalibrated IS systematics of Walker *et al.*<sup>29</sup> the corresponding shift can be written as

$$\delta E_{\text{IS}}/E_{\gamma} = (5.37 \pm 0.07) \times 10^{-12} (1 - \Delta V/V), \quad (5)$$

where  $\Delta V/V$  is the relative change in volume.

The constant  $\alpha$  in Eq. (4) was computed using (5) and the volume-change data reported by Shirane *et al.*<sup>5</sup> Figure 4 shows the variation of

$$c\delta E(T)_{\text{total}}/E_{\gamma} + (3k_B/2Mc - \alpha/E_{\gamma})T$$

in velocity units as a function of  $1/T$  ( $^{\circ}\text{K}^{-1}$ ).

Various interesting inferences can be drawn from the plot. In the first instance, it is seen that the variation is linear in the temperature range below  $450^{\circ}\text{C}$  (ferroelectric phase) and above  $540^{\circ}\text{C}$  (paraelectric phase). It is significant to point out that the above plot shows a discontinuous break in

$$\frac{c\delta E(T)_{\text{total}}}{E_{\gamma}} + \left(\frac{3k_B}{2Mc} - \frac{\alpha}{E_{\gamma}}\right)T$$

of  $0.075 \pm 0.04$  mm/sec at  $T_C$ . This sudden change may arise out of the discontinuous change in the IS because of sudden changes in volume at  $T_C$  and also due to changes in the nature of the chemical bond caused by the phase transition. Alternatively, the observed change may either be due to the change in the Debye temperature and/or to the disappearance of the soft mode. Assuming the values of the discontinuous volume changes at  $T_C$  as provided by Shirane's data<sup>5</sup> and using Eq. (5), it is estimated that the sudden changes in the IS at the transition temperature would be about 0.01 mm/sec. In addition to this there may be a slight change in the isomer shift because of the changes in the nature of the chemical bond caused by the phase transition. Thus

it appears that the origin of the discontinuous changes in  $\delta E_{\text{total}}$  has to be sought essentially in factors other than the isomer shift. There are three factors which can give rise to discontinuous changes in  $\delta E_{\text{total}}$  close to  $T_C$ . These are (a) changes in the Debye temperature on going through  $T_C$ , (b) the temperature dependence of the soft mode, and (c) the TA anomaly.<sup>10</sup> The last factor arises because of the optic-acoustic mode mixing for wave vector  $\vec{q}$  close to zero.<sup>10</sup> As a consequence of this mixing, the TA branch is pushed down in energy and shows anomalous temperature dependence.<sup>10</sup> Using Eq. (4), we can estimate the effect due to the change in the Debye temperature on crossing the Curie temperature. The calculations show that the difference in the Debye temperature on the two sides of  $T_C$  [if assumed to occur at  $T_C$  (see Sec. III C)] would give rise to a change in  $c\delta E(T)_{\text{total}}/E_\gamma$  of about 0.012 mm/sec. These calculations thus show clearly that the observed changes in  $\delta E_{\text{total}}$  on passing through  $T_C$  should essentially be due either to (i) soft mode or (ii) the TA anomaly. It is not possible to quantitatively determine the contributions of these two factors. It may also be of interest to point out that discontinuous changes in the center shift have been observed at ferromagnetic phase transitions<sup>30,31</sup> in Fe and also in the ferromagnetic bcc-to-hcp phase transition in Fe under high pressure.<sup>27</sup> Recently Wertheim *et al.*<sup>25</sup> have analyzed discontinuous changes in the center shift at the magnetic phase transition in FeF<sub>3</sub>. They attribute the changes in the center shift to the change in the Debye temperature as the temperature is raised through the transition temperature.

#### B. Electric Field Gradient

The IS studies have shown that the Mössbauer probe Fe<sup>57</sup> occupies the Ti<sup>4+</sup> site and has the Fe<sup>3+</sup> valence state. This is an S-state ion ( $3d^5$ ,  $^6S_{5/2}$ ) and has no field gradient of its own. Such a probe reflects faithfully the crystalline EFG. Figure 5 shows the variation of the quadrupole interaction  $\Delta E$  as a function of temperature. The disappearance of the quadrupole interaction at and above the transition temperature shows that the Mössbauer probe faithfully reflects the solid-state properties of the host lattice. In conformity with earlier studies<sup>12</sup> we find that although the Mössbauer probe is both a charge and a mass defect, it responds to and reflects the displacement of the Ti<sup>4+</sup> ion in the lattice. It is significant to note that  $\Delta E$  remains almost saturated till 320 °C. An increase in the temperature beyond this value causes a decrease in  $\Delta E$  which finally disappears at  $T_C$ . The quadrupole interaction  $\Delta E$  between the quadrupole moment  $eQ$  of the  $I = \frac{3}{2}$  state of the Fe<sup>57</sup> nucleus and the crystalline EFG ( $eq_L$ ), which is axially symmetric because of the tetragonal structure in the ferroelectric phase,

can be expressed as

$$\Delta E = \frac{1}{2}e^2q_LQ(1 - \gamma_\infty),$$

where  $\gamma_\infty$  is Sternheimer's antishielding factor. Using the recently determined values of  $\gamma_\infty = -0.14$ <sup>32</sup> and  $Q = 0.29b$ ,<sup>33</sup> we find that the lattice EFG is  $(7.35 \pm 0.04) \times 10^{13}$  esu cm<sup>-3</sup>. A comparison of these results with the earlier studies on the Mössbauer effect for Fe<sup>57</sup> in BaTiO<sub>3</sub><sup>12</sup> shows that the lattice EFG as measured in lead titanate is larger by a factor of  $1.41 \pm 0.04$  compared to that in BaTiO<sub>3</sub>. This is rather surprising in view of the fact that the tetragonal strain in PbTiO<sub>3</sub> is some six times that in BaTiO<sub>3</sub> and also in view of the observed sublattice shifts which are considerably larger than those in BaTiO<sub>3</sub>. The low ratio as well as the saturation of  $\Delta E$  below 320 °C indicate the saturation of the spontaneous polarization in this temperature range. It is interesting to mention that electric-quadrupole interaction has been investigated in polycrystalline PbTiO<sub>3</sub> by perturbed  $\gamma$ - $\gamma$  directional correlation of Sc<sup>44</sup>, Ti<sup>44</sup> being the parent isotope.<sup>34</sup> These authors also find that the ratio of the EFG at the Sc-ion site in PbTiO<sub>3</sub> is larger than that in BaTiO<sub>3</sub> by a factor  $1.46 \pm 0.07$ . The remarkable similarity between the perturbed-correlation studies and the present Mössbauer studies further reinforce our earlier inference that Fe occupies the Ti<sup>4+</sup> site and truly reflects the surrounding crystalline environment. Having seen that the ratios determined by the two techniques are nearly the same, one can now compare the EFG sensed by Sc<sup>3+</sup> (argon configuration) and Fe<sup>3+</sup> ( $3d^5$   $^6S_{5/2}$ ) in this lattice and thereby determine the antishielding factor for Sc<sup>44</sup>. Using EFG data for Sc and Fe, we find that the antishielding factor  $\gamma_\infty$  for Sc<sup>44</sup> is -19.

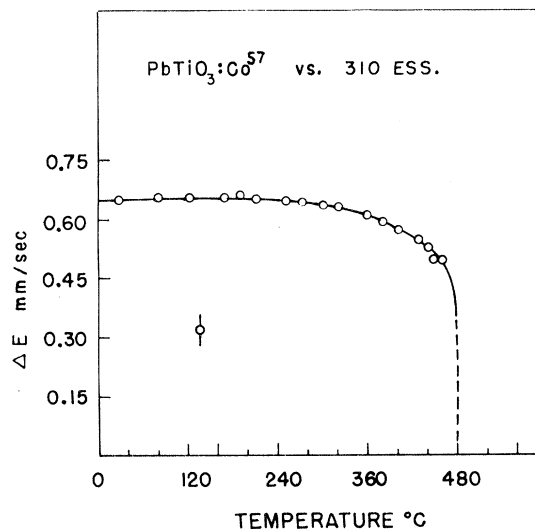


FIG. 5. Variation of the quadrupole splitting  $\Delta E$ , with temperature.

It may now be of interest to compare the experimentally observed value of the lattice EFG with the theoretically computed value. The lattice EFG is contributed by the monocharges in the lattice as well as by the dipoles at various lattice points. The former can be computed assuming the ionic model of the lattice and using the knowledge of ionic displacements and the lattice parameters obtained through the study of Shirane *et al.*<sup>5</sup> The dipolar contribution is obtained through internal-field calculations by Venevtsev *et al.*<sup>35</sup> These calculations give the electronic polarization and the dipole moment created at each of the ions in the lattice surrounding the Mössbauer probe. Using these data the computed lattice EFG is found to be  $32.5 \times 10^{13}$  esu cm<sup>-3</sup> as against the experimentally determined value of  $\sim 7.4 \times 10^{13}$  esu cm<sup>-3</sup>. This discrepancy might arise through the assumption of 100% ionicity in determining monopole contribution to the EFG. Alternatively, it might be that the lattice sum is not taken over a large enough number of unit cells or because of the neglect of the contributions to the lattice EFG by higher charge distribution (quadrupole and hexapole, etc.). Hewitt's<sup>36</sup> calculations in  $\text{KbO}_3$ , which give a very satisfactory approximation, have shown that the lattice EFG due to nearest-neighbor oxygen ions alone is close to the value calculated by summing over a large number of unit cells. Further it has been seen that the contribution to the EFG by higher charge distributions is negligibly small. If the assumption of 100% ionicity is the major source of discrepancy, then the discrepancy itself provides an estimate of the degree of ionicity. From this criterion the degree of ionicity in  $\text{PbTiO}_3$  is  $\sim 22\%$ . In  $\text{BaTiO}_3$  such an estimate provided the degree of ionicity of nearly 60%.<sup>12</sup> Following Triebwasser,<sup>37</sup> the ionicity computed from the knowledge of ionic displacement and ionic polarization in  $\text{PbTiO}_3$  comes to nearly 30%, whereas the value calculated by Triebwasser for  $\text{BaTiO}_3$ <sup>37</sup> is 45%. Using Danon's recalibrated IS systematics,<sup>25</sup> one can estimate the degree of ionicity through the effective charge on the central  $\text{Fe}^{3+}$  ion in the oxygen octahedra.<sup>38</sup> This analysis shows that the degree of ionicity in  $\text{BaTiO}_3$  and  $\text{PbTiO}_3$  is 27 and 20%, respectively, showing that  $\text{PbTiO}_3$  is more covalent than  $\text{BaTiO}_3$ , which is, in fact, expected because of drastic changes in the bond length and large sublattice shifts.

In  $\text{BaTiO}_3$  it was found that  $\Delta E$ ,  $P_s^2$  ( $P_s$  is the spontaneous polarization),<sup>12</sup> tetragonal strain, and birefringence<sup>39,40</sup> follow similar variation with temperature. However, in  $\text{PbTiO}_3$ ,  $\Delta E$ , tetragonal strain, and birefringence follow somewhat different variations with temperature (Fig. 6). It is seen that while  $\Delta E$  remains saturated until 320 °C, the birefringence  $n_c - n_a$  increases (absolutely) initially with temperature, reaches a maximum at about 400

°C, and decreases to zero at the transition temperature. If the polarizability of the surrounding oxygen ions in the  $\text{BO}_6$  octahedra is isotropic then it can be shown<sup>39,40</sup> that

$$(n_c - n_a) \propto (c - a)/a \propto P_s^2.$$

If, however, oxygen polarizabilities are not isotropic then the linearity between  $(n_c - n_a)$ ,  $[(c - a)/a]$  and  $P_s^2$  does not hold. Indeed, Lawless<sup>41</sup> has suggested that birefringence  $(n_c - n_a)$  is contributed by two factors, i. e., (i) the tetragonal strain and sublattice shifts and (ii) the anisotropy of the oxygen polarizability. The former increases the positive birefringence whereas the latter increases the negative birefringence, with decrease in the temperature. It appears that because of  $\text{Ti-O}_I$  overlap and the anisotropy in the oxygen polarizability,  $\Delta E$  has a somewhat different variation from that of  $(n_c - n_a)$ .

### C. Soft-Mode Behavior

It has been suggested by Cochran<sup>42</sup> and Anderson<sup>43</sup> that ferroelectricity in these perovskite ferroelectrics arises because of the existence of the temperature-dependent optical mode which decreases in frequency as the temperature of the crystal approaches the Curie temperature  $T_0$  from the high-temperature side. In the second-order ferroelectric phase transition, the disappearance of the optical mode brings in an instability leading to a phase transition at  $T_c$  which is equal to  $T_0$ . However, in the first-order phase transition, the instability sets in earlier because of the optic-acoustic mode mixing and the phase transition occurs at  $T_c$ , which is above  $T_0$ . In ferroelectrics undergoing either of the transitions, Mössbauer-effect studies provide a method for the detection of the temperature dependence of the soft mode.

The area  $A$  under the resonance curve after suitable corrections can be shown to be proportional to the Lamb-Mössbauer factor. Assuming a monatomic cubic lattice and the Debye model, the Lamb-Mössbauer factor  $f(T)$  can be expressed as<sup>44</sup>

$$f(T) = \exp \left\{ - \frac{E_\gamma^2}{2Mc^2} \frac{6}{k_B \Theta_D} \left[ \frac{1}{4} + \left( \frac{T}{\Theta_D} \right)^2 \int_0^{\Theta_D/T} \frac{x dx}{e^x - 1} \right] \right\}, \quad (6)$$

where  $\Theta_D$  is the Debye temperature,  $E_\gamma$  the transition energy of the 14.4-keV Mössbauer radiation, and  $k_B$  the Boltzmann constant. From this expression it is possible to determine the Debye temperature of the lattice from the knowledge of the temperature dependence of the Lamb-Mössbauer factor. Figure 7 shows the variation of the area under resonance (corrected suitably for background and normalized for off-resonance) as a function of temperature. This variation unequivocally shows the anomalous variation in the Lamb-Mössbauer factor in the vicinity of the transition temperature. In

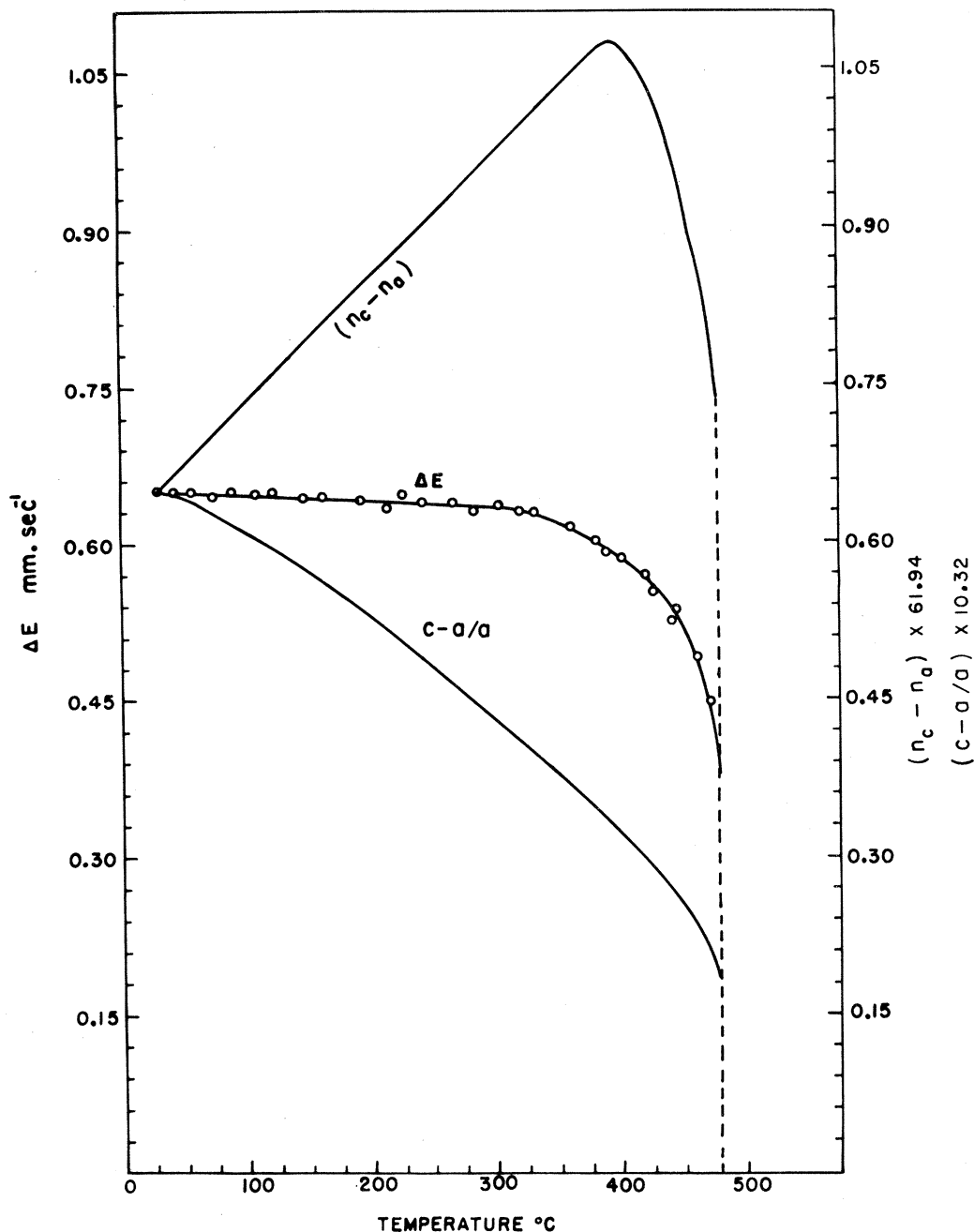


FIG. 6. Temperature variation of the quadrupole splitting  $\Delta E$ , birefringence  $n_c - n_a$  (Ref. 3), and the tetragonal strain  $[(c-a)/a]$  (Ref. 5). The solid lines indicate (on a matching scale) variation of  $(n_c - n_a)$  and  $[(c-a)/a]$ .

the temperature range much above the transition temperature, i. e., above  $650^\circ\text{C}$ , and much below the transition temperature, i. e., below  $350^\circ\text{C}$ , it is possible to estimate the Debye temperature of the lattice. By suitably fitting the temperature variation of the resonance area with the theoretically computed  $f$ -factor variations at various Debye temperature, it is found that the Debye temperature in

the high-temperature region, i. e., in the paraelectric phase, is about  $225^\circ\text{K}$ , whereas in the low-temperature region, i. e., in the ferroelectric phase, the Debye temperature is seen to be  $540^\circ\text{K}$  (Fig. 8). Thus it seems that on going through the ferroelectric transition, the Debye temperature decreases considerably. This may perhaps be due to piezoelectric and electroacoustic coupling which



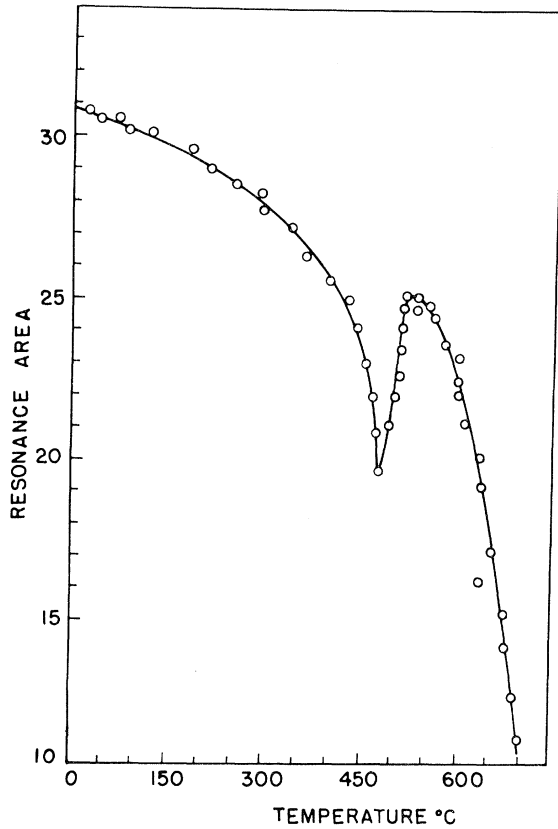


FIG. 7. Temperature variation of the normalized resonance area, showing a well-defined anomaly in the vicinity of  $T_C$ .

exist in the ferroelectric phase but disappear in the paraelectric phase.

The most striking feature of the variation of the area under resonance with temperature is that as one approaches  $T_C$  from both the low- and high-temperature sides, the area decreases and becomes minimum at  $T_C$ . The percentage reduction in the area under resonance at  $T_C$  is some 36% as opposed to 10% in  $\text{BaTiO}_3$ . The connection between the Lamb-Mössbauer factor and the temperature-dependent mode responsible for ferroelectricity in these perovskites was first suggested by Muziker *et al.*<sup>45</sup> and demonstrated experimentally by Bhide and Multani in the case of  $\text{BaTiO}_3$ .<sup>12</sup> However, in these investigations no attempt was made to obtain the analytical form for the Lamb-Mössbauer factor. We may now examine the observed variation in the area under resonance with temperature in the light of Cochran's lattice-dynamical theory of ferroelectricity. Cochran was the first to suggest an intimate connection between ferroelectricity in crystals and lattice dynamics. He suggested that the frequency of the temperature-dependent optical mode  $\omega_{an}$  varies as

$$\omega_{an}^2 = P(T - T_0),$$

where  $T_0$  is the Curie temperature. The existence of such soft modes in ferroelectrics has been confirmed by several authors using infrared neutron

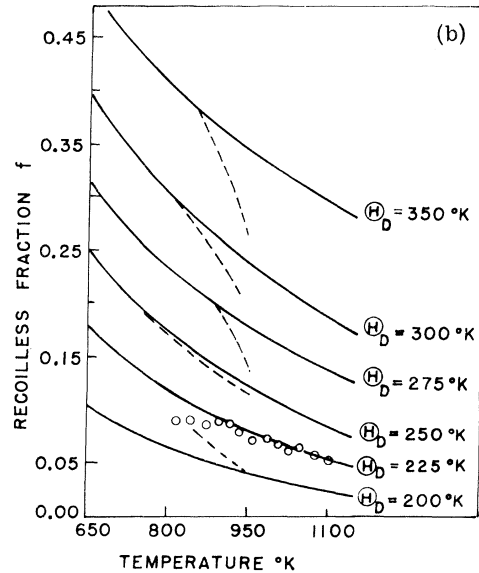
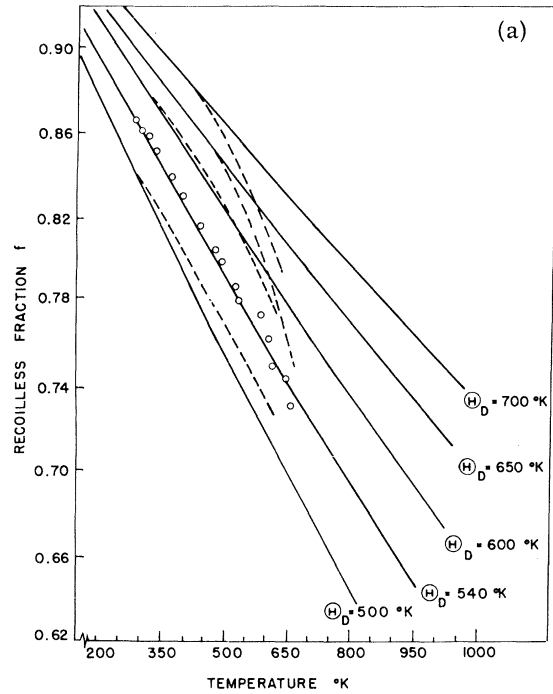


FIG. 8. Solid lines show the theoretical Lamb-Mössbauer factor for different Debye temperatures. Open circles and dashed lines represent the matched resonant fraction computed from the experimentally determined resonance area (a) below  $T_C$  and (b) above  $T_C$ , showing that the Debye temperature decreases considerably on crossing through  $T_C$ .

scattering and other experimental techniques.<sup>46,47</sup> The temperature-dependent mode will be reflected in the Mössbauer studies by a minimum in the recoilless fraction at the transition temperature. The Lamb-Mössbauer factor can be written

$$f(T) = \exp\left(-\sum_s \frac{(\hbar \vec{K})^2}{2M\hbar\omega_s} (2n_s + 1) \hat{\epsilon}_s^2\right), \quad (7)$$

where  $\omega_s$  is the lattice-mode frequency,  $\vec{K}$  is the  $\gamma$ -ray wave factor,  $M$  is the mass of the atom emitting Mössbauer radiation,  $\hat{\epsilon}_s$  is the polarization vector, and  $n_s$  is the phonon occupation number, which is given by

$$n_s = [\exp(\hbar\omega_s/k_B T) - 1]^{-1}.$$

For a monatomic lattice following the Debye model, Eq. (7) reduces to the well-known Lamb-Mössbauer factor [Eq. (6)]. If we postulate that one of the

modes has a temperature dependence as envisaged by Cochran,  $\omega_{an}^2 = P(T - T_0)$ , then the  $f$ -factor expression in Eq. (7) will be modified to the form

$$f(T) = \exp\left(-\sum_s \frac{(\hbar K)^2}{2M\hbar\omega_s} (2n_s + 1) \hat{\epsilon}_s^2\right) \times \exp\left(-\frac{(\hbar K)^2}{2M\hbar\omega_{an}} (2n_{an} + 1) \hat{\epsilon}_{an}^2\right). \quad (8)$$

Implied above is the assumption that the normal Debye-Waller factor is not much affected by taking the anomalous mode out of the summation. After substituting  $\omega_{an}^2 = P(T - T_0)$ , the above expression assumes the form

$$f(T) = \exp\left\{-\frac{E_\gamma^2}{2Mc^2} \frac{6}{k_B\Theta_D} \left[\frac{1}{4} + \left(\frac{T}{\Theta_D}\right)^2 \int_0^{\Theta_D/T} \frac{x dx}{e^x - 1}\right]\right\}$$

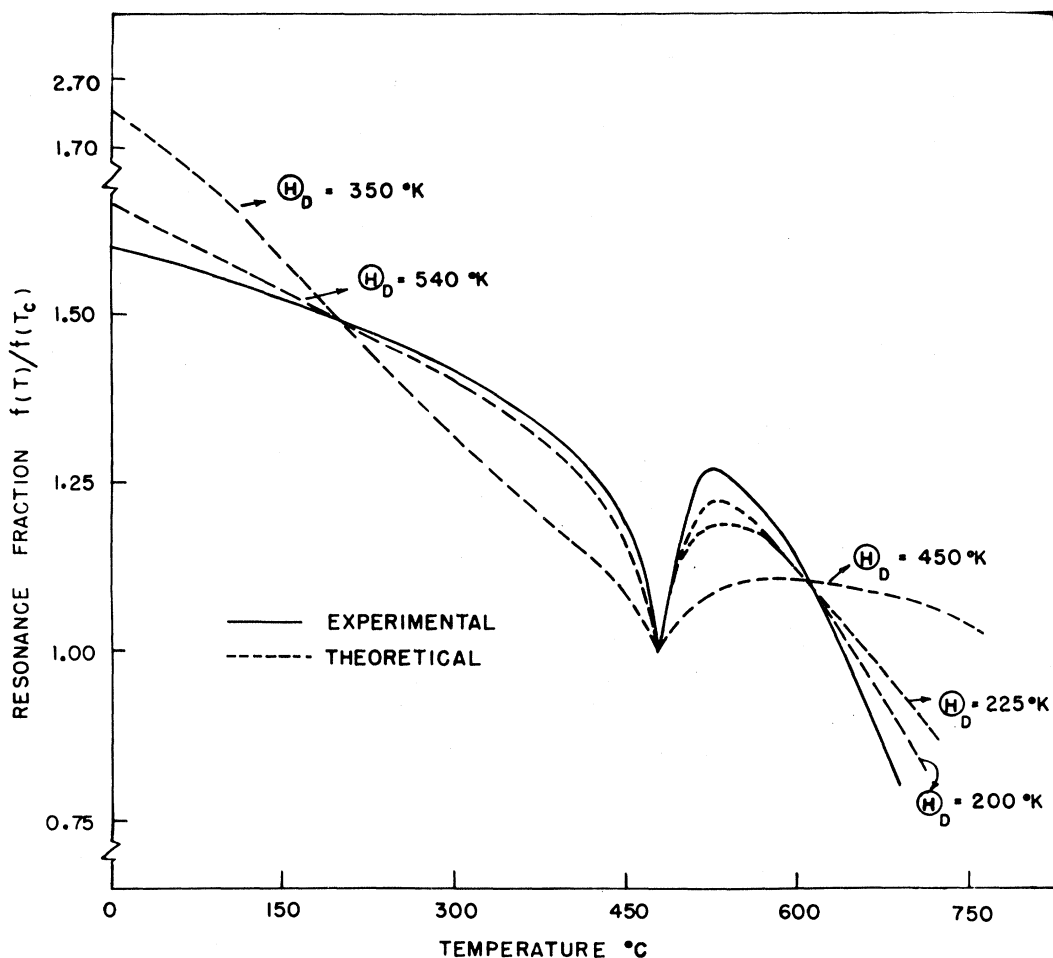


FIG. 9. Computer-fitted curves of the theoretical resonance fraction in the presence of Cochran-type optic mode at various temperatures, normalized to that at  $T_C$ , with the corresponding normalized area under resonance curve. The best fit obtained with  $\Theta_D(p) = 200^\circ\text{K}$ ,  $\Theta_D(f) = 540^\circ\text{K}$ ,  $T_0(p) = 703^\circ\text{K}$ ,  $T_0(f) = 973^\circ\text{K}$ ,  $P(p) = 0.13 \pm 0.03 \text{ meV}^2/^\circ\text{K}$ , and  $T_C = 753^\circ\text{K}$  shows the essential validity of the soft-mode behavior suggested by Cochran.

$$\times \exp \left[ - \left( \frac{2}{\exp \left\{ \frac{\hbar [P(T - T_0)]^{1/2} / k_B T}{\hbar} \right\} - 1} + 1 \right) \times \left( \frac{(\hbar K)^2}{2M \hbar [P(T - T_0)]^{1/2}} \hat{\epsilon}_{an}^2 \right) \right]. \quad (9)$$

From this expression it is immediately seen that for a second-order transition,  $f(T)$  goes to zero as  $T \rightarrow T_0 (= T_C)$ . However, for a first-order transition, the crystal becomes unstable at the transition temperature  $T_C$  even before  $T_0$  is reached and one can express

$$\omega_{an}^2 = P(T - T_C) + P(T_C - T_0).$$

Substituting this value of  $\omega_{an}^2$  in Eq. (9), it is seen that even for a first-order transition, the Lamb-Mössbauer factor will have a minimum at  $T_C$ .

There are a number of parameters which need to be known to determine  $f(T)$  at any temperature. These parameters are  $\Theta_D$ ,  $\hat{\epsilon}_{an}^2$ ,  $P$ ,  $T_0$ , and the transition temperature  $T_C$ . It is quite likely that  $\Theta_D$ ,  $\hat{\epsilon}_{an}^2$ ,  $P$ , and  $T_0$  may have different values below and above the transition temperature. Thus there are nine unknown quantities. Fortunately our Mössbauer studies provide  $\Theta_D(p)$  and  $\Theta_D(f)$  from the Lamb-Mössbauer factor variations. Similarly,  $T_0(p)$ ,  $T_0(f)$ , and  $T_C$  were taken to be 430, 520, and 480 °C, respectively. [The symbols ( $p$ ) and ( $f$ ) indicate the respective values as computed from the behavior in the paraelectric and ferroelectric phases, respectively.] We are thus left with four unknown quantities  $P(p)$ ,  $\epsilon_{an}^2(p)$ ,  $P(f)$ , and  $\epsilon_{an}^2(f)$ . Shirane's data on neutron scattering<sup>10</sup> provide  $P(p) = 0.13 \pm 0.03 \text{ meV}^2/\text{°K}$ . Using these values the theoretical curves were fitted to the experimental curves to obtain  $\epsilon_{an}^2(p)$ . In order to make comparison between theoretical and experimental values, both  $f(T)$  and the experimentally observed area under resonance were normalized with re-

spect to the corresponding values at  $T_C$ . The ratio  $A(T)/A(T_C)$  of the areas gives the ratio of  $f$  factors at the two temperatures. After achieving the best fit in the paraelectric phase, and thereby obtaining  $\epsilon_{an}^2(p)$ , an attempt was made to achieve the best fit in the ferroelectric phase by choosing different values of  $\epsilon_{an}^2(f)$  and  $P(f)$ . During these computations it was seen that  $f(T)/f(T_C)$  is not very sensitive to  $\epsilon_{an}^2$  and hence in subsequent computations  $\epsilon_{an}^2(f)$  has been taken to be equal to  $\epsilon_{an}^2(p)$ . We find that using  $\epsilon_{an}^2(f) = \epsilon_{an}^2(p)$  a best fit is obtained for  $P = 0.30 \text{ meV}^2/\text{°K}$ . Although different combinations of  $\Theta_D(p)$ ,  $\Theta_D(f)$ , etc., were tried, only a few curves including the curve giving the best fit are shown in Fig. 9. It is interesting to point out that if one uses the computed value of  $P(f)$  to determine the frequency of the  $\vec{q} = 0$  mode at room temperature, one obtains the mode energy of 12.35 meV. This value agrees reasonably well with that reported by Perry *et al.*<sup>48</sup> (10.3 meV) from their infrared studies and with that reported by Shirane *et al.*<sup>10</sup> from their neutron-scattering experiments. In all these fittings it has been assumed that the Debye temperature changes discontinuously at  $T_C$ . It is more than likely that the  $\Theta_D$  in the vicinity of the transition temperature may itself be temperature dependent. The exact computation and fitting with experimental results would require information on this aspect. However, to a first approximation, it appears that Cochran's suggested dependence of the soft mode explains the observed variation of the Lamb-Mössbauer factor.

#### ACKNOWLEDGMENTS

One of us (M. S. H.) wishes to thank the University Grants Commission and the Council of Scientific and Industrial Research, New Delhi, for the financial support which made this work possible.

<sup>1</sup>For an excellent review, see F. Jona and G. Shirane, *Ferroelectric Crystals* (Pergamon, New York, 1962), Chaps. IV and V.

<sup>2</sup>J. Kobayashi and R. Ueda, *Phys. Rev.* **99**, 1900 (1955); J. Kobayashi, S. Okamoto, and R. Ueda, *ibid.* **103**, 830 (1956).

<sup>3</sup>G. Shirane, R. Pepinsky, and B. C. Frazer, *Acta Cryst.* **9**, 131 (1956).

<sup>4</sup>M. S. Hegde, M. S. thesis (Bombay University, 1964), Chap. III, pp. 135 and 136 (unpublished).

<sup>5</sup>G. Shirane and Sadao Hoshino, *J. Phys. Soc. Japan* **6**, 265 (1951).

<sup>6</sup>H. D. Megaw, *Proc. Roy. Soc. (London)* **189**, 261 (1947).

<sup>7</sup>V. G. Bhide, K. G. Deshmukh, and M. S. Hedge, *Physica* **28**, 871 (1962).

<sup>8</sup>V. G. Bhide, M. S. Hegde, and K. G. Deshmukh, *J. Am. Ceram. Soc.* **51**, 565 (1968).

<sup>9</sup>J. P. Remeika and A. M. Glass, *Mater. Res. Bull.*

**5**, 37 (1970).

<sup>10</sup>G. Shirane, J. D. Axe, and J. Harada, *Phys. Rev. B* **2**, 155 (1970).

<sup>11</sup>V. G. Bhide and M. S. Hegde (unpublished).

<sup>12</sup>V. G. Bhide and M. S. Multani, *Phys. Rev.* **139**, A1983 (1965).

<sup>13</sup>V. G. Bhide and M. S. Multani, *Phys. Rev.* **149**, 289 (1966).

<sup>14</sup>M. DiDomenico, Jr., S. H. Wemble, S. P. S. Porto, and R. F. Bauman, *Phys. Rev.* **174**, 522 (1968).

<sup>15</sup>Y. Yamada, G. Shirane, and A. Linz, *Phys. Rev.* **177**, 848 (1969).

<sup>16</sup>A. Nishioka, K. Sekikawa, and M. Owaki, *J. Phys. Soc. Japan* **11**, 181 (1957).

<sup>17</sup>V. G. Bhide and M. S. Hegde (unpublished).

<sup>18</sup>J. D. Hurd, A. W. Simpson, and R. H. Tredgold, *Proc. Phys. Soc. (London)* **73**, 448 (1959).

<sup>19</sup>A. Yu. Kudzins, *Kristallografiya* **7**, 799, (1962) [*Sov. Phys. Crist.* **7**, 646 (1963)].

- <sup>20</sup>K. A. Muller, in *Paramagnetic Resonance*, edited by W. Low (Academic, New York, 1963), Vol. I.
- <sup>21</sup>A. W. Hornig, R. C. Rempel, and H. E. Weaver, *J. Phys. Chem. Solids* **10**, 1 (1959).
- <sup>22</sup>V. G. Bhide and H. C. Bhasin, *Phys. Rev.* **159**, 586 (1967).
- <sup>23</sup>D. J. A. Gainon, *Phys. Rev.* **134**, A1300 (1964).
- <sup>24</sup>E. Simanek and Z. Sroubek, *Phys. Rev.* **163**, 275 (1967).
- <sup>25</sup>G. K. Wertheim, D. N. E. Buchman, and H. J. Guggenheim, *Phys. Rev. B* **2**, 1392 (1970).
- <sup>26</sup>R. V. Pound, G. B. Benedek, and R. Drever, *Phys. Rev. Letters* **1**, 405 (1961).
- <sup>27</sup>D. N. Pipkorn, C. K. Edge, P. Debrunner, G. Depasquali, H. G. Drickmer, and H. Fraunfelder, *Phys. Rev.* **135**, A1604 (1964); Ref. 38, p. 171.
- <sup>28</sup>J. Danon, Intern. At. Energy Agency Tech. Rept. Ser. **50**, 89 (1966).
- <sup>29</sup>L. R. Walker, G. K. Wertheim, and V. Jaccarino, *Phys. Rev. Letters* **6**, 98 (1961).
- <sup>30</sup>R. S. Preston, S. S. Hanna, and J. Heberle, *Phys. Rev.* **128**, 2207 (1962).
- <sup>31</sup>T. A. Kovats and J. C. Walker, *Phys. Rev.* **181**, 610 (1969).
- <sup>32</sup>R. M. Sternheimer, *Phys. Rev.* **130**, 1423 (1963).
- <sup>33</sup>R. Ingalls, *Phys. Rev.* **133**, A787 (1964).
- <sup>34</sup>M. R. Haas and J. C. Glass (unpublished).
- <sup>35</sup>Yu. Venevtsev *et al.*, *Kristallografiya* **3**, 473 (1958); **4**, 255 (1959).
- <sup>36</sup>R. R. Hewitt, *Phys. Rev.* **121**, 45 (1961).
- <sup>37</sup>S. J. Triebwasser, *J. Phys. Chem. Solids* **3**, 53 (1957).
- <sup>38</sup>J. Danon, *Chemical Applications of Mössbauer Spectroscopy*, edited by V. I. Goldanskii and R. H. Herber (Academic, New York, 1968), p. 173.
- <sup>39</sup>W. J. Merz, *Phys. Rev.* **76**, 1221 (1949).
- <sup>40</sup>For an excellent discussion see Ref. 1, pp. 121, 122, and 145-147.
- <sup>41</sup>W. N. Lawless, *Phys. Rev.* **138**, A1751 (1965).
- <sup>42</sup>W. Cochran, *Phys. Rev. Letters* **3**, 412 (1959); *Advan. Phys.* **9**, 387 (1960); **10**, 401 (1961).
- <sup>43</sup>P. W. Anderson, *Fizika Dielektrikov AN. SSSR*, **290** (1960).
- <sup>44</sup>G. K. Wertheim, *Mössbauer Effect: Principles and Applications* (Academic, New York, 1964).
- <sup>45</sup>C. Muzikar, J. V. Janovec, and V. Dvorak, *Phys. Status Solidi* **3**, K9 (1963).
- <sup>46</sup>See, for example, references given in G. Shirane, J. P. Axe, and J. Harada, *Phys. Rev. B* **2**, 3651 (1970); Kensuke Tani, *J. Phys. Soc. Japan* **26**, 93 (1969).
- <sup>47</sup>E. Fatuzzo and W. J. Merz, in *Selected Topics in Solid State Physics*, edited by E. P. Wohlfarth (North-Holland, Amsterdam, 1967), Vol. VII.
- <sup>48</sup>C. H. Perry, B. N. Khanna, and G. Rupprecht, *Phys. Rev.* **135**, A408 (1964).

## Electron-Nuclear-Double-Resonance and Electron-Spin-Resonance Evidence for a Fe<sup>3+</sup> (K<sup>+</sup> Vacancy) Center in Iron-Doped KZnF<sub>3</sub>

J. J. Krebs and R. K. Jeck\*†

Naval Research Laboratory, Washington, D. C. 20390

(Received 3 January 1972)

Crystals of KZnF<sub>3</sub> doped with  $\geq 0.05$ -at. % iron exhibit Fe<sup>3+</sup> electron-spin-resonance (ESR) and electron-nuclear-double-resonance (ENDOR) spectra which indicate the existence of a charge compensator along a  $\langle 111 \rangle$  direction. This is over and above the cubic spectrum observed at lower doping levels. The ESR spin-Hamiltonian parameters of the compensated center at 77 °K are  $a = +49.7(4)$ ,  $D = +107.9(3)$ , and  $F = -2.7(4)$  (in units of  $10^{-4}$  cm<sup>-1</sup>) and  $g = 2.0029(3)$ . The angular ENDOR data for the two sets of three nearest-neighbor fluorines were analyzed to determine the local distortion in some detail. The results are in good accord with a model which assumes that one of the eight nearest-neighbor K<sup>+</sup> ions surrounding the Fe<sup>3+</sup> is absent.

### INTRODUCTION

The transferred hyperfine interactions of the transition-metal ions Mn<sup>2+</sup>, Fe<sup>3+</sup>, Co<sup>2+</sup>, and Ni<sup>2+</sup> located in the cubic Zn<sup>2+</sup> sites in the perovskite fluoride KZnF<sub>3</sub> have recently been investigated.<sup>1</sup> During the course of this work, electron-spin-resonance (ESR) spectra characterized by maximum splitting for H<sub>||</sub> $\langle 111 \rangle$  were found in iron-doped KZnF<sub>3</sub> crystals and these same samples exhibited <sup>19</sup>F electron-nuclear-double-resonance (ENDOR) lines which were clearly not associated with Fe<sup>3+</sup> in cubic

sites. In this paper, we report a thorough-going ESR/ENDOR investigation of these spectra and their source—designated as the Fe-(111) center. The characteristics of this center are in substantial agreement with a model involving a nearest-neighbor (nn) K<sup>+</sup> vacancy which locally charge compensates the Fe<sup>3+</sup> ion. The experiment serves as an excellent example of the power of the ENDOR technique in obtaining detailed information about transition-metal ions in sites lacking local stoichiometry. Such information is, in large measure, unattainable from the ESR spectra of these centers.